SENSORLESS FLUX REGION MODIFICATION OF DTC CONTROLLED IM FOR TORQUE RIPPLE REDUCTION

Yavuz USER[1], Kayhan GULEZ[2], Sukru OZEN[1]

[1] Electric Electronic Engineering, University of Akdeniz, Antalya,Turkey
[2] Control ve Automation Engineering, University of Yıldız Technic, Istanbul,Turkey
yuser@akdeniz.edu.tr, gulez@yildiz.edu.tr, sukruozen@akdeniz.edu.tr

Abstract: *A Direct Torque Control (DTC) drive allows direct and independent control of flux linkage and electromagnetic torque by the selection of optimum inverter switching tables. There is no need for any complex transformation of current or voltage. However, each vector selected from the switching table cannot produce the required accurate stator voltage vector to provide the desired torque and flux. This results in the production of ripples in the torque as well as flux waveforms. In this study, we propose a method to reduce torque and flux fluctuations. In this method, the flux region of conventional DTC model are modificated and is compared to conventional DTC method. Speed is estimated from MRAS. The conventional MRAS-based sensorless DTC and the flux region modification method are simulated and the comparison of their practice performances is presented.*

Keywords: *Induction motor, Direct torque control, Flux Region modification method, MRAS, Torque and Flux Linkage ripple.*

1. Introduction

Induction motors are widely used in the industry due to their simple form and low maintenance need. Many different methods have been tried to control the induction motors. For years, the induction motor control market is dominated by the vector control methods. However, the latest trend is the development of the direct torque control (DTC) because it is simple, fast and more advantageous [2],[5]. The direct control method is sufficient to control with respect to changes in the machine parameters without using reverse current regulation in addition to providing fast dynamic torque response. The Direct Torque Control strategy does not require axes transformation and voltage decoupling blocks [1].

However, the generation of only six non-zero voltage vectors by the voltage source inverter is a drawback. The required torque is met for only few switching instants and mostly the generated voltage vectors produce a torque that is either more or less than the required torque. As a result, ripples are generated in the torque as well as flux waveforms [6].Increasing the inverter switching frequency by a space vector modulation scheme is proposed for the torque ripple reduction [7]-[8]. The concept of dead beat controller is used to increase the switching frequency. But this approach introduces complexity.

In this study, sensorless flux region modification of DTC method will be introduced. First, we will illustrate conventional DTC. Then, the concept of torque ripple reduction method will be discussed. The switching table for the selection of optimum voltage vector, MRAS speed estimation schema and balance equations will be presented. The simulated ve experimental results will be given for comparing the performance of the basic sensorless scheme and the new sensorless scheme.

2. Conventional DTC Method

Direct torque control method (DTC) is based on applying a switching series, which shall directly eliminate errors, which shall occur in torque,

Received on: 30.12.2013
Accepted on: 05.03.2014

through the reference given as value and the calculated flux, to the power switching elements in the inverter [10],[11],[15]. Other vector control methods are mostly based on rotor flux while DTC method is based on stator flux.

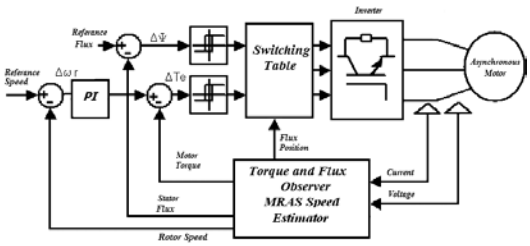

Figure 1. Direct torque control method block diagram

This may be realized by using motor model on the fixed α-β axis set. Stator flux, torque and stator flux sector zone may be calculated with the help of currents and voltages measured in the motor's stator as the following [9].

$$v_{s\alpha} = R_s i_{s\alpha} + \frac{d\psi_{s\alpha}}{dt} \tag{1}$$

$$v_{s\beta} = R_s i_{s\beta} + \frac{d\psi_{s\beta}}{dt} \tag{2}$$

$$T_e = p\left(i_{s\alpha} i_{s\beta} - i_{s\beta} i_{s\alpha}\right) \tag{3}$$

$$\psi_{s\alpha} = \int \left(v_{s\alpha} - R_s\, i_{s\alpha}\right) dt \tag{4}$$

$$\psi_{s\beta} = \int \left(v_{s\beta} - R_s\, i_{s\beta}\right) dt \tag{5}$$

$$\left|\vec{\psi}_s\right| = \sqrt{\left(\psi_{s\alpha}^2 + \psi_{s\beta}^2\right)} \tag{6}$$

Herein, Rs is stator phase resistance, p is the number of pole couple, isα, isβ, ψsα, ψsβ, Vsα, Vsβ are current , flux and voltage values on the axis of α-β, Te is momentum. Amplitude of the vector of the torque and the stator flux calculated with the help of the above equations. The reference value of the stator flux magnitude is compared with the actual flux magnitude. The error obtained is given to a two-level hysteresis comparator. If the error is positive, it implies that the flux magnitude has to be increased and this is denoted as dψ=1. If the error is negative, it implies that the flux magnitude has to be decreased and this is denoted as dψ=0. The flux comparator conditions are given as

$$\begin{aligned} d\psi &= 1 \ \text{ for } \left|\psi_{ref}\right| - \left|\psi_s\right| \geq \left|\Delta\psi_s / 2\right| \\ d\psi &= 0 \ \text{ for } \left|\psi_{ref}\right| - \left|\psi_s\right| \geq \left|\Delta\psi_s / 2\right| \end{aligned} \tag{8}$$

The rotor reference speed is compared with the feedback speed and by a suitable PI controller this error is converted into reference torque. The reference torque is compared with the real torque and the error obtained is fed to a three-level hysteresis comparator. If the error is positive, it implies that the torque has to be increased and this is denoted by dt_e=1. If the error is negative, it implies the torque has to be reduced and this is denoted by dt_e= -1. It the error is zero, it implies the torque needs to be constant and this is denoted by dte=0. The torque comparator conditions are given as

$$dt_e = 1 \quad \text{for } \left|t_{ref}\right| - \left|t_e\right| \geq \left|\Delta t_e / 2\right| \tag{9}$$

$$dt_e = -1 \ \text{for} \quad \left|t_{ref}\right| - \left|t_e\right| \leq \left|-\Delta t_e / 2\right| \tag{10}$$

$$dt_e = 0 \quad \text{for } \left|-\Delta t_e / 2\right| \leq \left|t_{ref}\right| - \left|t_e\right| \leq \left|\Delta t_e / 2\right| \tag{11}$$

To accomplish optimum switching process, one of the 8 different voltage vectors consisting of 8 different switching is selected as seen in Figure 2. Vi (Sa, Sb, Sc) (i=0,1,2…7) Besides 6 switching levels, there are V_0(0,0,0) and V_7(1,1,1) levels not producing a voltage at the output when they are applied [4].

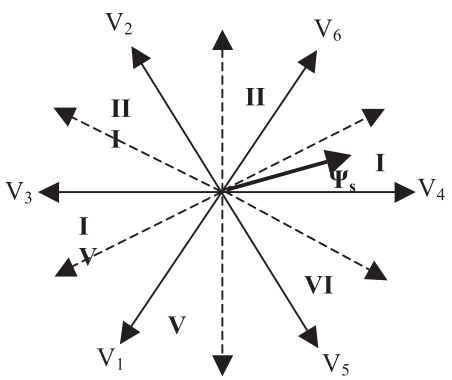

Figure 2. Voltage Space Vector and Sector Representation

Assuming the stator flux linkage space vector to be in sector I and is rotating in counter clockwise direction, the resultant effect of generating different voltage vectors at this instant is given in the Figure 3.

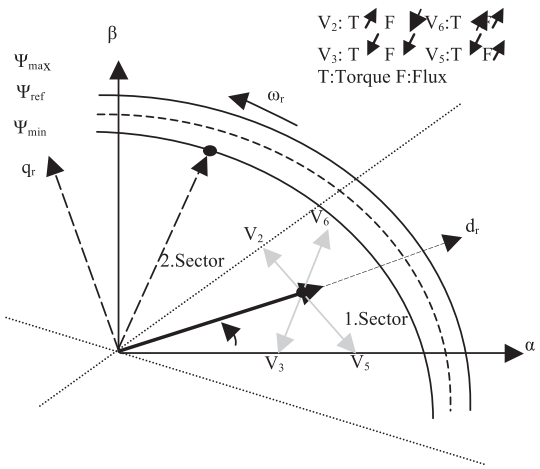

Figure 3. Voltage Space Vector for Flux and Torque Variation

Table 1, which is seen below, shows switching logics when the motor is desired to counter clockwise.

Table 1. Optimal Switching Logics For Rotating Couter Clockwise

		θ(1)	θ(2)	θ(3)	θ(4)	θ(5)	θ(6)
$d\psi$ =0	dt_e=1	V_5	V_1	V_3	V_2	V_6	V_4
	dt_e=0	V_7	V_0	V_7	V_0	V_7	V_0
	dt_e=-	V_6	V_4	V_5	V_1	V_3	V_2
$d\psi$=1	dt_e=1	V_1	V_3	V_2	V_6	V_4	V_5
	dt_e=0	V_0	V_7	V_0	V_7	V_0	V_7
	dt_e=-	V_2	V_6	V_4	V_5	V_1	V_3

3. Flux Region Modification Strategy

In the conventional DTC, although flux is expected to increase in the harmonic during the sector change, it could decrease below the limits of a hysteresis band. Particularly in low speed, the stator flux amplitude moves beyond the flux band interval in every sector change. In order to solve this problem, we propose a method where an angle for the stator flux sector is chosen prior to the sector change. In this method, the flux sector is rotated and the active voltage vector of the previous sector is applied for a while even though the voltage space vector is in a new sector. Therefore, the required stator flux amplitude could be achieved. In Figure 4, we present the new sector formation after rotating first and second sector for a 30 degree[16]. In the conventional DTC, the selection of the voltage vectors depends on only two outputs of the hysteresis control (dψs and dte) and the angle of the stator flux space vector (Position of θs).

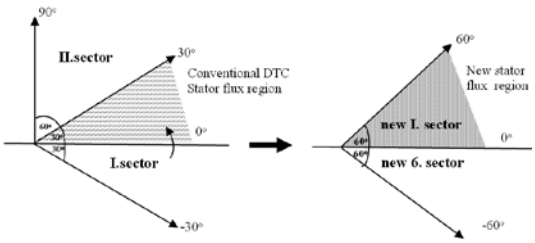

Figure 4. The stator flux regions in the conventional and rotated DTC

In the method, the relationship between the d axis of the voltage vector applied with outputs of hysteresis control, vd and its tangent q axis component, vq is defined. According to this relationship, if vd>0, the stator flux amplitude will increase and at the same time if vq>0, the torque will rapidly increase as well. Similar to Figure 3, let the stator flux space vector be initially at A0 and moving counter-clockwise. Then, the flux amplitude is at the lower limit of the hysteresis band. In order to increase the flux amplitude, V2 vector should be selected. When V2 is applied, the position of the stator flux will move to A1. However, the reference value for the flux amplitude has not been achieved yet and there is no other voltage vector that could be applied for achieving that value. This is due to the fact that the Vd component of applied voltage vector at the flux is too small. Since the Vq component is large at the same time, the torque rapidly increases. In the conventional DTC, the output of the torque hysteresis control with same condition provides dt=0. As shown in Table 1, the controller selects zero voltage vector and as a result, the flux amplitude drops to the lower values. Creating new flux regions could prevent the decrease in flux at the lower speed[17]. The flux, initially at A1, does not decrease and the flux space vector will move from A1 to A2 as seen in Figure 3. Thus, the decrease in flux is prevented. Table 2 presents new switching table produced by the rotated flux regions.

4. Model Referance Adaptive System (MRAS)

The MRAS technique is used in sensorless IM drivers, at the first time, by Schauder[14]. Figure 5 since this, it has been a topic of many applications [1].

Table 2. Modified Switching Logics For Rotating Couter Clockwise

		θ(1)	θ(2)	θ(3)	θ(4)	θ(5)	θ(6)
$d\psi_s$=0	dt_e=1	V_6	V_2	V_3	V_1	V_5	V_4
	dt_e=0	V_7	V_0	V_7	V_0	V_7	V_0
	dt_e=-1	V_4	V_6	V_2	V_3	V_1	V_5
$d\psi_s$=1	dt_e=1	V_3	V_1	V_5	V_4	V_6	V_2
	dt_e=0	V_0	V_7	V_0	V_7	V_0	V_7
	dt_e=-1	V_1	V_5	V_4	V_6	V_2	V_3

In a MRAS system, some state variables, xd, xq (e.g. rotor flux-linkage components, ψrα , ψrβ or back e.m.f. components, ed , eq , etc.) of the induction machine (which are obtained by using measured quantities, e.g. stator voltages and currents) are estimated in a reference model and are then compared with state variables estimated by using an adaptive model. The difference between these state variables is then used in an adaptation mechanism, which outputs the estimated value of the rotor speed (ωr) and adjusts the adaptive model until satisfactory performance is obtained. Such a scheme is shown in Fig. 5 where the actual implementation, and here the components of the space vectors are shown. The adaptation mechanism in the Figure 5 is a PI controller[15].

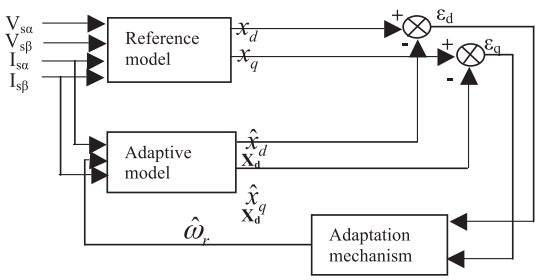

Figure 5. MRAS-based basic speed estimator scheme

3.1. Rotor Speed Estimator

The rotor speed can be estimated by using two types of estimators (a reference-model-based estimator and an adaptive-model- based one), They independently determine the rotor flux-linkage components in the stator reference frame ($\psi_{r\alpha}$, $\psi_{r\beta}$), and the difference between these flux-linkage estimates are used to drive the speed of the adaptive model. The rotor flux linkages in the stationary reference frame can be obtained by using the stator voltage and current equations of the induction machine in the stationary reference frame. These equations are shown below:

Reference Model:

$$\psi_{r\alpha} = \frac{L_r}{L_m}\left[\int(v_{s\alpha} - R_s i_{s\alpha})dt - L_s' i_{s\alpha}\right] \quad (16)$$

$$\psi_{r\beta} = \frac{L_r}{L_m}\left[\int(v_{s\beta} - R_s i_{s\beta})dt - L_s' i_{s\beta}\right] \quad (17)$$

Adaptive Model:

$$\hat{\psi}_{r\alpha} = \frac{1}{T_r}\int(L_m i_{s\alpha} - \hat{\psi}_{r\alpha} - \omega_r T_r \hat{\psi}_{r\beta})dt \quad (18)$$

$$\hat{\psi}_{r\beta} = \frac{1}{T_r}\int(L_m i_{s\beta} - \hat{\psi}_{r\beta} - \omega_r T_r \hat{\psi}_{r\alpha})dt \quad (19)$$

Herein, Tr is rotor time constant, Ls is stator circuit leakage inductance, Lr is rotor circuit reduced leakage inductance, Lm is magnetization inductance. The reference and adaptive models are used to estimate the rotor flux – linkages and the angular difference of the outputs of the two estimators $\varepsilon_\omega = \mathrm{Im}(\psi_r \hat{\psi}_r) = \psi_{r\beta}\hat{\psi}_{r\alpha} - \psi_{r\alpha}\hat{\psi}_{r\beta}$ is used as the speed tuning signal. This tuning signal is the input to a linear controller (PI controller) which outputs the estimated rotor speed as shown in Figure 6.

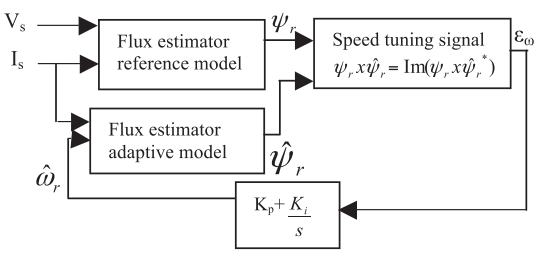

Figure 6. MRAS-based rotor speed observer flux linkages for the speed tuning signal

When the rotor speed to be estimated (ω_r) is changed in the adjustable model in such a way that the difference between the output of the reference model and the output of the adjustable model becomes zero, then the estimated rotor speed is equal to the actual rotor speed (ω_r) The error signal actuates the rotor-speed identification algorithm, which makes this error converge to zero. Estimated speed can be expressed as

$$\hat{\omega}_r = K_p \varepsilon_\omega + K_i \int \varepsilon_\omega dt \quad (20)$$

Arbitrary K_p and K_i cannot be used obtain satisfactory performance in this equation. The complete scheme of the flux based MRAS rotor speed observer is shown in Fig.7

In the next sections, we present the simulation and experimental results of the conventional DTC without a sensor and the new method without a sensor and compare their performance.

5. Simulation Results

We simulate the conventional DTC and the DTC without a sensor where the flux regions are rotated and compare the results. Figures 8-13 present the transient and steady-state results. Speed reduction is acquired with MRAS and it is observed to be within the reference speed values.

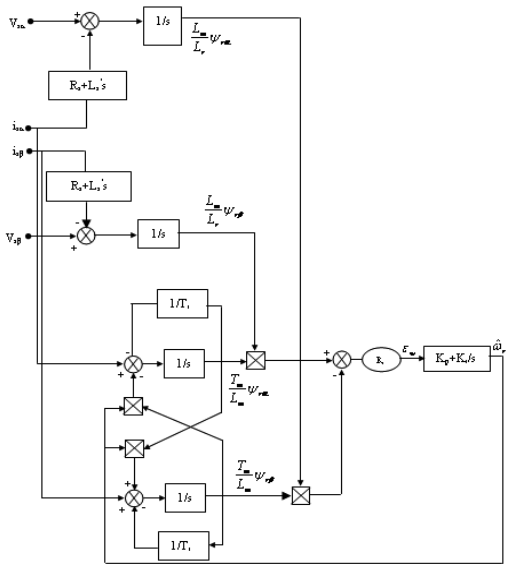

Figure 7. Complete schema of MRAS speed observer using rotor flux linkages

In the steady-state, high amplitude ripple disappear. The number of oscillations in current and voltage waves is decreased. Comparing the conventional DTC and DTC using the rotated flux regions without a sensor, the new method provides significant reduction in the flux and torque.

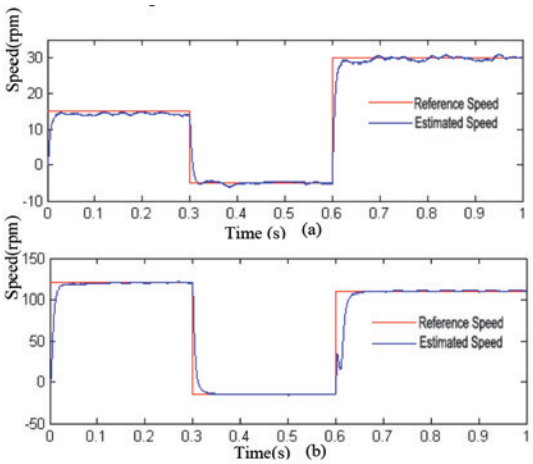

Figure 8. Estimated rotor speed (a)15 rpm, -5 rpm, 30 rpm (b)120 rpm, -15 rpm, 110 rpm

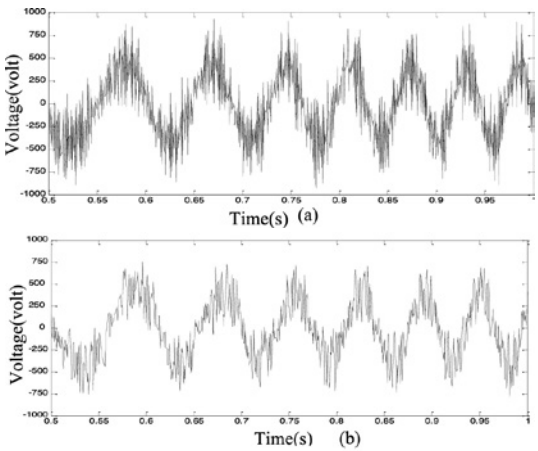

Figure 9. Stator phese voltage V_{ab} a)Conventional (b) Proposed DTC

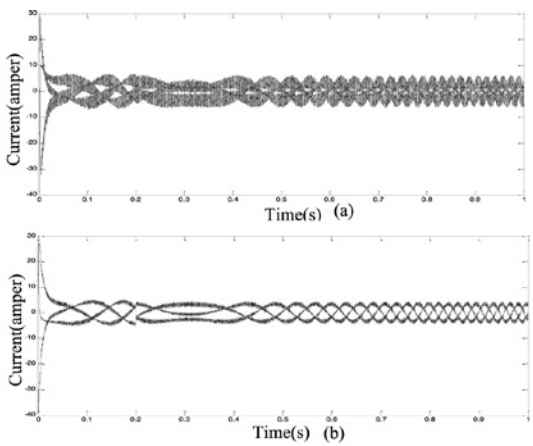

Figure 10. Stator phase currents I_{abc} (a)Conventional (b)Proposed DTC

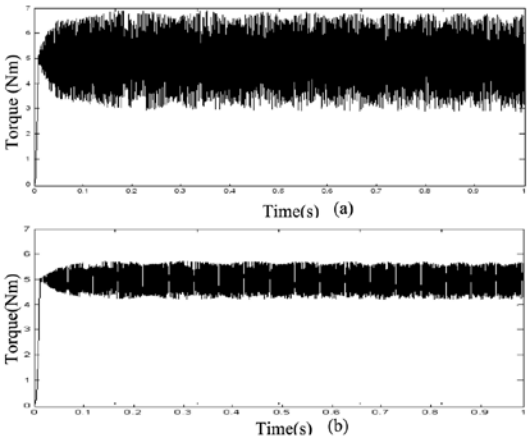

Figure 11. Electromagnetic torque (a)Conventional (b) Proposed DTC

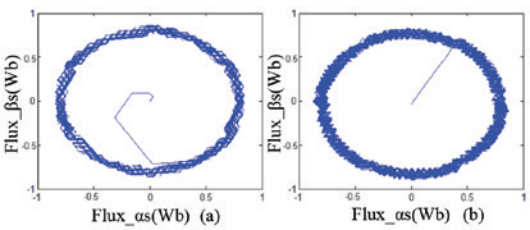

Figure 12. Stator flux locus (a)Conventional (b) Proposed DTC

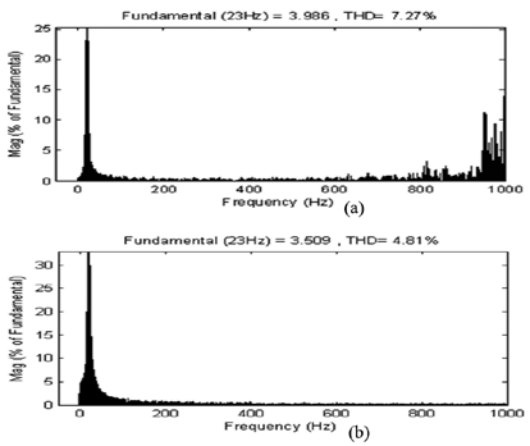

Figure 13. Spectrum of stator current phase A (a) Conventional(b)Proposed DTC

6. Experimental Setup

Figure 14 shows the block scheme of the experimental setup. In the experimental setup, each unit is created separately. Then, they are connected to each other. The experimental setup consists of AC-DC engine unit, PC-SCSI communication port, DC-Link capacitor unit, IPM inverter unit, current and voltage circuit unit, reference current and voltage circuit unit, feedback circuit unit and optic isolation unit.

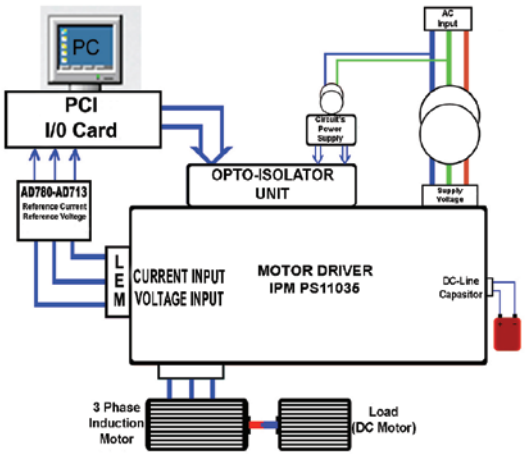

Figure 14. The block schematic of the experimental setup

In the algorithm, necessary voltage and current information from the sensors are obtained using the PCI I/O card. PCI card has 16 analog and digital input channels and 16 digital output channels. Out of all analog input channels, three are used for determining the current and voltage; seven are used for the digital output channel inverter and the control of the inverter signal. Extra information about AC motor and Load motor could be found in Appendix-A. Figure 15 presents the realization of the experimental setup.

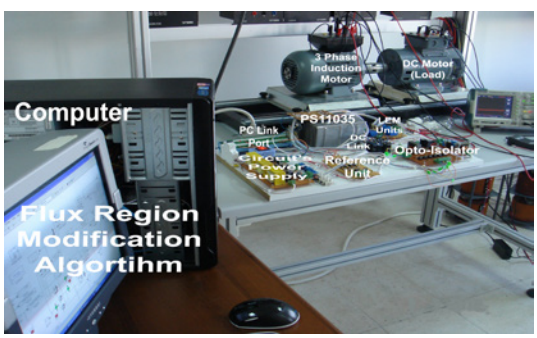

Figure 15. Realization of the experimental setup

6.1. Experimental Results

Next figures 16-19 present the transient and steady-state analyses of experimental results.

Figure 16. Stator phese voltage V_{ab} (a)Conventional (b)Proposed DTC

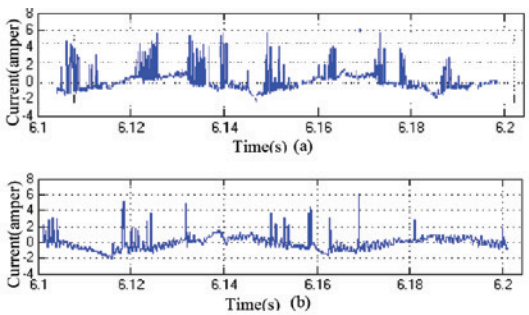

Figure 17. Stator phase currents I_{abc} (a)Conventional (b)Proposed DTC

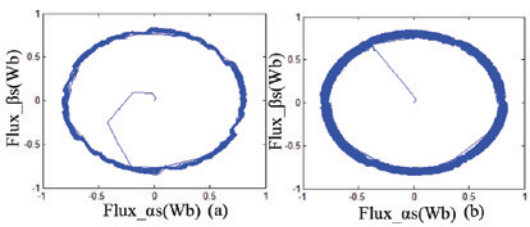

Figure 18. Stator flux locus (a)Conventional (b)Proposed DTC

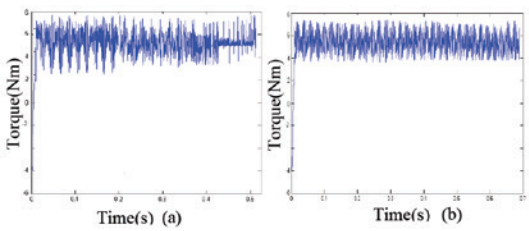

Figure 19. Electromagnetic torque (a)Conventional (b)Proposed DTC

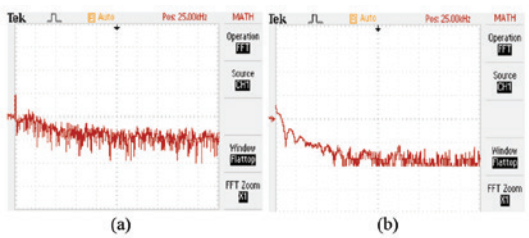

Figure 19. EMI noise level (a)Conventional (b) Proposed DTC

7. Results

In this study, we eliminate the use of the external sensor. We explored the flux regions of the conventional DTC method and proposed to rotate the flux regions in order to reduce torque ripple. Speed reduction is determined with flux based MRAS and both methods are compared with respect to current, voltage, flux and torque. The proposed method provides significant reduction in a phase current and voltage in the simulation and experimental results. Torque ripple is reduced by about 1/3 Nm with the new method. In addition, the reference flux values are obtained and the flux ripple is reduced by 0.8 Wb compared to the conventional DTC. We present the screen of the spectrum analyzer which is connected to the motor a phase. Without the new method, the current harmonics are around 7.3 % THD and 1 kHz. After applying the new method, THD is decreased to 4.8 % and harmonics around 1 kHz are disappeared. The results suggest that the flux and torque ripple are reduced by rotating the flux regions and adjusting the switching table. Speed, reduced using MRAS, is close enough to the reference speed.

8. References

[1] X.Li, R. Duke and S. Round., "Development of a three-phase three-level inverter for an electric vehicle", Australasian Universities PowerEngineering Conf., 1999, Darwin, Australia, pp. 247-251.

[2] Sarıoglu M. K., "Fundamentals of Electric Machines I", ITU, Faculty of Electric- Electronic, Ofset Press Room,3.Press, 1984.

[3] Sarıoglu M.K., "Gokasan M., Bogosyan S.,Asynchronous Machines and it's Control", Birsen Publishing, ISBN 975-511-343-6, 2003.

[4] Vasudevan M., Arumugam R., "New Direct Torque Control Scheme of Induction Motor for Electric Vehicles".

[5] Parekh R., "AC Induction Motor Fundamentals", Microchip Technology Inc., AN887,U.S.A., 2003.

[6] Luukko, J., "Direct Torque Control of Permanent Magnet Synchronous Machines -Analysis and Implementation", Diss. Lappeenranta University of Technology, Lappeenranta, Stockholm, 2000.

[7] Okumuş, H.,İ., "Improved Direct Torque Control of Induction Machine Drives", PhD Thesis, University of Bristol, July, UK, 2001.

[8] Mei, C.G., Panda, S.K., Xu, J.X. ve Lim, K.W., "Direct Torque Control of Induction Motor-Variable Switching Sectors", Proc. of the 3rd Power Electronics and Drive Systems, Proceedings of the IEEE International Conference, 1999, 1:80-85.

[9] Schauder, C., "Adaptive Speed identification for vector control of induction motors without rotational transducers", IEEE Tran.Ind. Applic., 5(IA-22): 965-970, 1999.

[10] Cirrincione, M. and M. Pucci, "Sensorless direct torque control of an induction motor by a TLS-based MRAS observer with adaptive integration", Automatica, 11(41): 1843-1854, 2005.

[11] Kojabali,H.M., L. Chang and R. Doraismi, "A MRAS based adaptive pseudo-reduced order flux observer for sensorless induction motor drivers", Elec. Power Components Systems, 4(20):930-937, 2005.

[12] Kraiem,H.,Ben Hamed,M., Sbita, L. ve Naceuraldulkrim, M., "DTC Sensorless Induction Motor Drives Based on MRAS Simultaneous Estimation of Rotor Speed Stator Resistance" ,International Journal of Electrical and Power Engineering, 2(5):306-313,2008.

[13] SIMULINK Dynamic System Simulation for MATLAB Modeling, Simulation, Implementation, The MathWorks, Inc. Natick, Massachusetts,USA,2010.

[14] Schauder, C. 1992. Adaptive Speed identification for vector control of induction motors without rotational transducers. IEEE. Tran. Ind.Applic.,5(IA-22): 965-970.

[15] User Y., Gulez K., Ozen S., "Sensorless Twelve Sector Implementation of DTC Controlled IM for Torque Ripple Reduction", 6th International Advaced Technoloqies Symposium, pp. 317-321, May 2011.

[16] Y. S. Lai, J. H. Chen, "A new approach to direct torque control of induction motor drives for constant inverter switching frequency and torque ripple reduction, IEEE Trans.Energy Conversion, vol. 16, pp. 220-227, Sept. 2001.

[17] T. G. Habetler, F. Profumo, M. Pastorelli and L. M. Tolbert, "Direct torque control of induction machines using space vector modulation," IEEE Trans. Industrial Applications, vol. 28, pp.1045-1053, Sept/Oct 1992.

ACKNOWLEDGMENT

The research has been supported by the Research Project Department of Akdeniz University, Antalya, Turkey.

APPENDIX A

Hereinafter are given IM parameters, reference values and sampling period.

Ts=100μs, T_L=2Nm, ψ_{ref}=0.8Wb, PI: Kp=90, Ki=0.5, $\Delta\psi_s$=±0.05V.s/rad Δt_e=±0.08Nm.

P_{mek}=3000W, R_r=1,93, R_s=1,45, L_s=12,2.10^{-3}h, L_r= 0.19734, R_r=1.45, L_m=0,1878 , p=2, J=0,03 Kgm^2, T_r=Lr/Rr.

APPENDIX B

Herinafter is given complete schema of sensorless direct torque control.

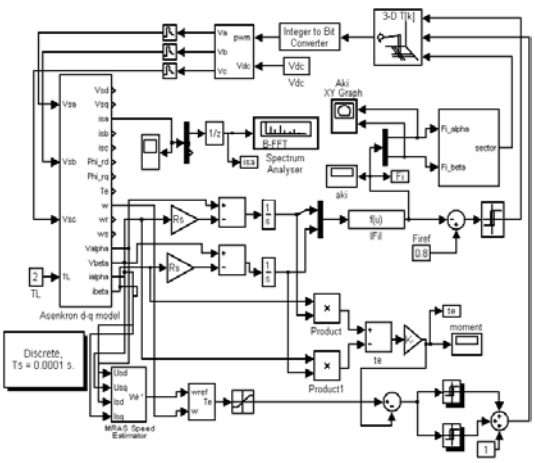

Yavuz User He received the B.S. degree in Electronic and Communication engineering from Kocaeli University, Kocaeli, Turkey and the M.S. degree in Electric engineering from Sakarya University, Sakarya, Turkey, in 1999 and 2004 respectively. He received the Ph.D. degree in control and automation engineering from Yildiz Technical University, Istanbul, Turkey, in

2012. From 1998 to 2000, he was a member of the technical staff of an electric company. In 2000, he joined the Department of Electric, Electronics Science in Vocational High School , University of Akdeniz, and worked as an Instructor in Industrial Electronic Program between 2000 and 2014. He is currently Associate Professor of Electric and Electronic Engineering at the University of Akdeniz. His research interests are in the field of electric machines and drives, which include modeling and identification of ac machines, control of ac and dc motors, industry applications of the power electronics and electric converters.

Kayhan Gulez Kayhan Gulez is Associate Professor of Control and Automation Engineering at the Yildiz Technical University since 2010. He received his B.S., M.S., and Ph.D. degrees all in Electrical Engineering from Yildiz Technical University, Istanbul, Turkey. He joined and worked in the Department of Electrical Engineering at Yildiz Technical University between 1997 and 2010. He worked as a Research Associate in a JSPS project and other short-term projects in Keio University and in Tokyo Metropolitan Institute of Technology between 1999 and 2002. His major research interests are Electrical Vehicle and Unmanned Air Vehicle Applications, Intelligent based Control Systems, Sensor Network Control Problems, EMC and EMI Control Methods, Active, Passive and EMI Filter Design Methods and Applications for EMI Noise and Harmonic Problems on which he has over 200 scientific papers and technical reports in various journals and conference proceedings. He has been serving as a reviewer and program committee member to numerous journals and conferences in these areas. He has also 9 science grand awards between 1998 and 2009 and The Superior Success Science Award in 2009 in Yildiz Technical University in Istanbul, and best paper awards from SCI'2001, M&S'2001 and TOK.

Sukru Ozen was born in Antalya, Turkey, in 1971. He received the engineering from the University of Yıldız Technical and Ph.D. degrees from the University of Sakarya, Turkey, in 1992 and 2003, respectively. He is Associate Professor of Electrical Engineering at the University of Akdeniz. Since 1998, he has been engaged in studies on the biological effects of electromagnetic fields, including studies on mechanisms of interaction and biomedical applications. His research interests also include electromagnetic compatibility, wave propagations, numerical methods, electromagnetic compatibility, signal processing, applied electromagnetic and biomedical engineering problems.